VNIR OPTICAL CONSTANTS FOR A DIVERSE SUITE OF CARBONATE MINERALS. A. M. Zastrow[1], C. Ye[2], E. C. Sklute and T. D. Glotch[1], [1]Stony Brook University, Stony Brook NY, USA (allison.zastrow@stonybrook.edu), [2]Northern Arizona University, Flagstaff, AZ, USA, [3]Planetary Science Institute, Tucson, AZ, USA.

Introduction: Visible to near-infrared (VNIR) spectroscopy is an incredibly important and useful tool for the identification and characterization of minerals and mineral assemblages across planetary bodies. Of particular interest is the potential to quantitatively analyze remote sensing VNIR reflectance data that cover a wide area (e.g., the 18 m/pixel spatial resolution of the Compact Reconnaissance Imaging Spectrometer for Mars (CRISM) targeted images [1]) and therefore likely contain a combination of minerals over that area. Thus, the spectra gathered by remote sensing instruments reflect mixtures of minerals that we would like to deconvolve into its endmember abundances.

This spectral unmixing is often done by employing radiative transfer theory, which requires knowledge of the real and imaginary indices of refraction (*n* and *k*, respectively) for the minerals of interest, which are also often referred to as optical constants. Using these optical constants for a mineral, paired with a chosen grain size, the bulk single scattering albedo (SSA) can be determined. From there, SSA spectra can be combined linearly to produce spectra that match the remote sensing data. Unfortunately, optical constants have not yet been derived for many minerals.

To facilitate more accurate modeling of carbonate-bearing areas on Mars, we are building on the library of optical constants presented in [2 and 3] to include a suite of carbonate minerals: calcite (Ca-carbonate), aragonite (Ca-carbonate), magnesite (Mg-carbonate), siderite (Fe-carbonate), and rhodochrosite (Mn-carbonate). We are using the MATLAB code documented in [4]. In this abstract, we present preliminary *n* and *k* results for calcite.

Samples and Data Collection:

Sample preparation: Each of the samples was sieved into three size fractions: 45-63 µm, 63-90 µm, and 90-125 µm. The samples were crushed into powder using a mortar and pestle and then dry-sieved into the three size fractions. After the initial sieving, the samples were dry-sieved once more before being washed with pure ethanol to remove residual fines. After drying the samples were dry-sieved one last time to verify the size fractionation.

VNIR data collection: VNIR spectra were collected using the ASD FieldSpec3 Max spectrometer at Stony Brook University. The incidence angle of the light (*i*) was held constant at 45°, while the emergence angle (*e*) varied from 0° to -60° at 10° intervals, resulting in the following phase angles ($g = i + |e|$): 45°, 55°, 65°, 75°, 85°, 95°, and 105°. The sample was held a constant distance away from both the light source and detector at every angle. We optimized the detector and gathered a white reference for every angle and sample. As an improvement on the setup described in [2 and 3], we have added a small table that spins at a constant rate of 4 revolutions per minute to acquire a more accurate mean sample spectrum compared to the previous protocol of manually rotating the sample cup four times during data collection.

Data calibration: After collection, the data were corrected to account for changes in the absolute reflectance of the Spectralon standard over time and according to [5] to correct for photometric effects of the Spectralon standard.

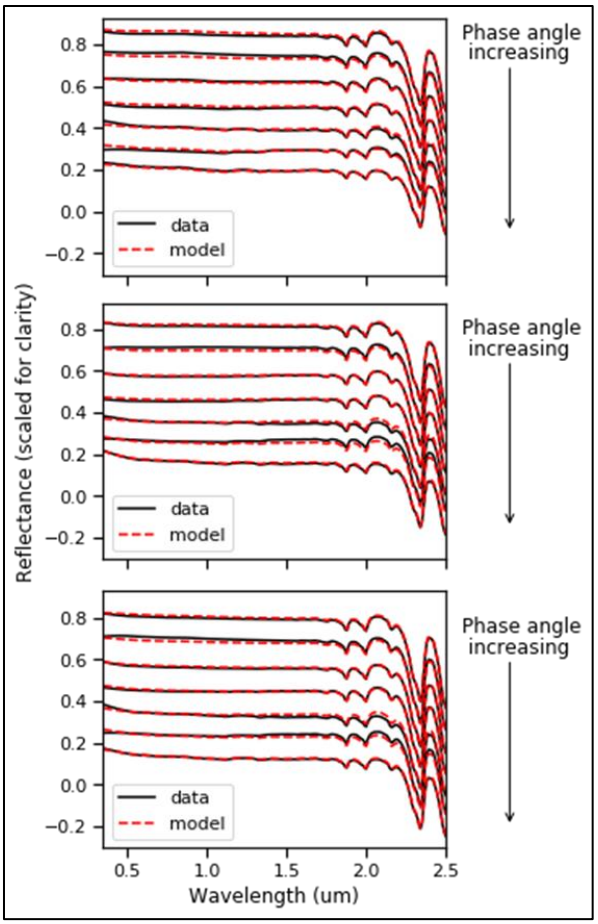

Figure 1: Model results compared to data. Top: small grain size, middle: medium grain size, bottom: large grain size.

Optical Constant Calculation: The calculation of optical constants presented in [2, 3] is based on the Hapke model of radiative transfer theory [6, 7] which accounts for a variety of physical properties for a target material such as grain size, composition, and porosity, as well as experimental setup parameters such as the phase angle between the incident light and emergence angle of the detector as noted above.

The code base follows an iterative pattern to calculate *n* and *k* given the inputs of laboratory-measured VNIR spectra for a sample at multiple grain size fractions and multiple phase angles (3 and 7, respectively, in this work). An initial *n* value is provided by the measured refractive index at the sodium D line at ~589 nm, but the model considers *n* to be wavelength-dependent across the entire spectrum.

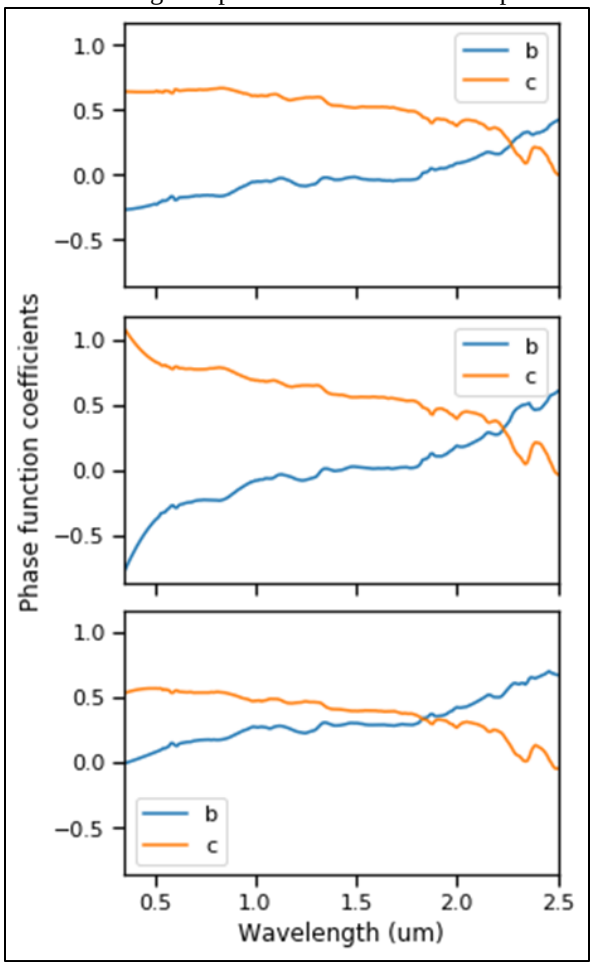

Figure 2: Phase function coefficients *b* & *c* for the small (top), medium (middle), and large (bottom) grain sizes. *b* is the degree of forward- and back-scattering and *c* is the degree of side-scattering. Positive *b* values indicate back-scattering.

[2] found that the inclusion of mid-infrared (MIR) spectra greatly increased the accuracy of the optical constant derivation, and so the final data input to the model are estimated MIR optical constants for the mineral. We have used the MIR optical constants published by [8], which were calculated using classical Lorentz-Lorenz dispersion theory.

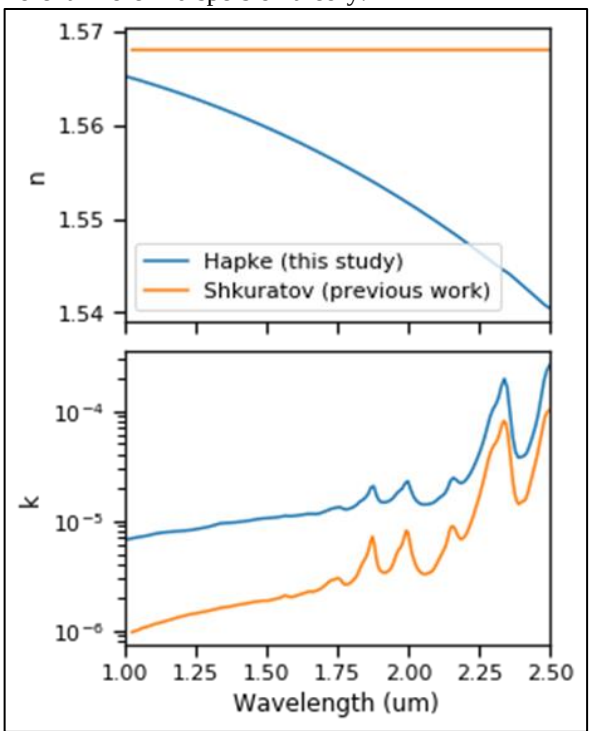

Figure 3: Model results *n* and *k*.

Preliminary Results: Preliminary *n* and *k* results for calcite are presented here and are also compared to previous optical constants derived using the Shkuratov model [9] which were used in spectral mixture analysis of CRISM data over Jezero Crater, Mars [10]. The Shkuratov model does not account for any differences in phase angle and these results were only derived using one grain size. Additionally, MIR data are not incorporated into the derivation, so the Shkuratov-based *k* values are lower and the *n* values do not vary with wavelength like the Hapke-based *n* values do.

Acknowledgments: This research was funded by NASA's Mars Data Analysis Program, Award #80NSSC18K1372. The MATLAB code used in this work can be found at zenodo.org/record/4429127.

References: [1] Murchie, S. et al., (2007) *JGR, 112*, E05S03. [2] Sklute, E. C. et al. (2015) *Am. Mineral., 100*, 1110-1122. [3] Ye, C. et al. (2021) *Earth and Space Sci., 8*. [4] Sklute, E. C. et al. (2021) *LPS LII*, Abstract #1258. [5] Yang, Y. et al., (2019) *JGR-Planets, 124*(1), 31-60. [6] Hapke, B. (1981) *JGR, 86*, 3039-3054. [7] Hapke, B. (2012) Cambridge University Press, UK, 507p. [8] Lane, M. D. (1999) *JGR, 104*, 14099-14108. [9] Shkuratov, Y. et al., (1999), *Icarus, 137*(2), 235-246. [10] Zastrow, A. M. and Glotch, T. D., (2021), *GRL, 48*(9).